

# PRESENT PERFORMANCE AND FUTURE REQUIREMENTS OF THE RF SYSTEMS FOR THE FERMI PROJECT

G. D’Auria\*, P. Craievich, M. Ferianis, M. Milloch, Sincrotrone Trieste, Trieste, Italy  
 L. Doolittle, A. Ratti, LBNL, Berkeley, California, U.S.A.  
 D. Cheever, T. Zwart, MIT-Bates, Middleton, Massachusetts, U.S.A.

## Abstract

The VUV soft x-ray FEL user facility, FERMI@ELETTRA, will use the existing 1.2 GeV linac to produce, in two separate phases, 100-40 nm and 40-10 nm, intense photon beams with single stage and double stage harmonic generation schemes respectively. To fulfill the stringent requirements of the project the present RF systems will be completely revised and upgraded. The work presented here describes the present performance of the system and plans for the linac upgrades to meet the required system specifications for FEL operation.

## 1. INTRODUCTION

The FERMI@ELETTRA project aims at developing a single-pass FEL user facility covering the spectral range 100-40 nm and 40-10 nm. A complete description of the project can be found in [1] and the main machine parameters for the two different phases are summarized in Table 1. The electron source will be the 1.2 GeV linac currently used as the injector for ELETTRA [2], modified in the layout and fully revised and upgraded in its RF system. The machine layout proposed for FERMI is reported in Figure (1). A detailed discussion of the optimization procedures adopted in this scheme can be found in [3].

Table 1: FEL main parameters

Parameter	FEL I	FEL II
Wavelength (nm)	100 - 40	40 - 10
Beam energy (GeV)	1.2	
Bunch charge (nC)	0.33 – 1.0	
Uncorrelated energy spread (%)	1.3 E-4	
Slice emittance (mm-mrad)	1.2	
Usable bunch length (fs)	200 – 800	

Seven additional RF accelerating structures, provided by CERN after the LIL decommissioning, will be installed in the low energy part of the machine to accelerate and prepare the beam before and after the first

bunch compressor. A new electron source, consisting of a high brilliance photoinjector (LCLS type scaled to 2998 MHz) [4], will inject into the renewed linac. This means that the FERMI linac will be composed of three different accelerating structures:

- the existing, SLAC type, 3.2 m long constant impedance sections (S0A-S0B);
- the seven new modules from CERN, 4.5 m long, constant gradient, SLAC type (C1-C7);
- the seven existing high gradient structures, 6.1 m long, constant impedance, SLED equipped, with nose cone and a reduced beam aperture (S1-S7).

A detailed description of the above mentioned components and their characterization in terms of impedance and wake fields can be found in [5].

The new layout also includes two bunch compressors, to increase the peak current from the 80 A generated at gun up to the required 1 kA. We are also evaluating the need for a fourth harmonic X-band structure to linearize the charge inside the bunch before the first bunch compressor.

Particularly important for the machine development and upgrade is the realization of the new machine front end at low energy, i.e., from the photoinjector to the first bunch compressor, that will be implemented as soon as possible in a new machine tunnel located upstream the present one [6]. In this paper we report the present status of the RF systems, the phase stability measurements carried out on four of them, and a preliminary layout of the new RF distribution with a study of the RF tolerances allowed to properly operate the FEL.

## 2. RF SYSTEM

### System Layout and Performance

The present RF system is based on eight high power modulators, capable of 102 MW peak power and operated at 10 Hz, with their own klystron (Thales TH 2132A, 3 GHz, 45 MW peak power, 4.5 μsec pulse width). The configuration adopted for each power station is based on an 18-cell PFN (Guillemin type E Pulse Forming Network), resonant charged with a constant current HV power supply (FUG-HCK 6750M-30000), and discharged

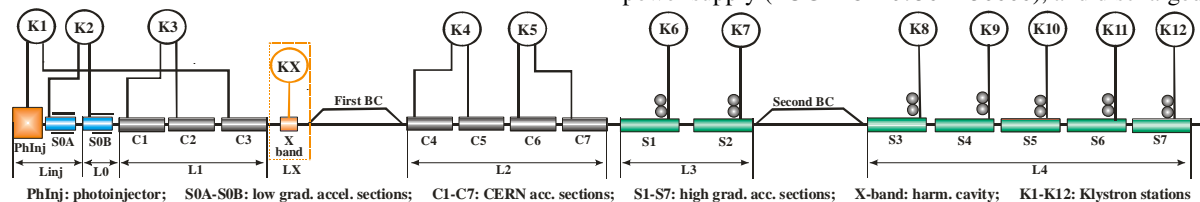


Figure 1: FERMI machine layout

\*gerardo.dauria@elettra.trieste.it

with a double gap thyratron (EEV CX 1536X). The use of a coupled inductance PFN optimizes the rectangular pulse shape at the output compared to a conventional L-C network with the same number of elements.

The need to power seven supplementary accelerating sections, C1-C7, will bring the total number of FERMI RF systems from eight to twelve. If we were to adopt the linearizer system, it would require an X-band plant. Figure 1 shows the scheme of the whole RF distribution for the new machine layout, note that only the section S1-S7 will be fed through the existing SLED system. Table 2 summarizes the expected energy gain per section and the energy budget for the whole machine assuming that each klystron will operate at about 40 MW and a 3.5 μsec pulse length, leaving an operating margin on the maximum available gradient per structure between 10% to 20%.

Table 2: Linac energy budget

Type of structure	Qt	ΔE (MeV)	Energy gain on crest (MeV)
Gun	1	5	5
S0A – S0B	2	45	90
C1 – C7	7	47	329
S1 – S7	7	120	840
<b>Total energy gain</b>			<b>1264</b>
For 1.2 GeV at the linac exit ΔE <sub>max</sub> = 64 MeV/5.0%			

*System modeling*

From the proposed layout for FERMI, we performed LiTrack [7] studies to evaluate the RF systems sensitivity and required tolerances in terms of amplitude and phase variations, for the extreme case of the FEL-1 short pulse (200 fs). In this case, we divided the linac in the sectors L0...L4, as shown in Fig.1, grouping the RF systems before and after the bunch compressors.

Table 3 shows the rms values of the required tolerance of the various stations, in terms of RF amplitude and phase, in order to simultaneously keep at the linac output a pulse-to-pulse energy variation below 10%, an energy jitter smaller than 0.1% and a time jitter on the bunch arrival less than 200 fs. The calculated values need to be further reduced by 1/√N, where N is the total number of klystrons per sector.

Using the same machine layout, we studied the beam optimization with and without the X-band section downstream the first bunch compressor, in order to understand the importance of the linearizing system. Table 3 summarizes the tolerance required with and without the X-band system and, for any parameter, we have highlighted in bold the requested value and in brackets the more stringent requirements asked by the case without the linearizing section. This exercise shows the effectiveness of the X-band system in relaxing the requirements for amplitude and phase stability of the main system, in particular for the stations installed before

the first bunch compressor. The gradients and RF phases assumed in this study are listed in Table 4.

Table 3: RF tolerance budget

With X-band (without X-band)					
Parameter	Symbol	ΔI/I <sub>0</sub>   <10%	ΔE/E <sub>0</sub>   <0.1%	Δt  <200 fs	Unit
L0	φ0	<b>0.30</b>	0.9 (0.30)	1.88 (0.9)	deg
L1	φ1	<b>0.19</b>	0.2 ( <b>0.18</b> )	0.19	deg
LX	φx	<b>0.30</b>	0.30	0.30	deg
L2	φ2	0.5 (0.18)	<b>0.18</b>	0.18	deg
L3	φ3	0.30	<b>0.18</b>	0.18	deg
L4	φ4	1.00	<b>0.50</b>	2.67	deg
L0	DV <sub>0</sub> /V <sub>0</sub>	<b>0.30</b>	0.86 ( <b>0.15</b> )	0.30	%
L1	DV <sub>1</sub> /V <sub>1</sub>	0.3 (0.18)	<b>0.29 (0.15)</b>	0.29 (0.18)	%
LX	DV <sub>x</sub> /V <sub>x</sub>	<b>0.30</b>	3.63	0.30	%
L2	DV <sub>2</sub> /V <sub>2</sub>	0.40	<b>0.18 (0.15)</b>	0.18	%
L3	DV <sub>3</sub> /V <sub>3</sub>	0.35	<b>0.18 (0.15)</b>	0.18	%
L4	DV <sub>4</sub> /V <sub>4</sub>	2.70	<b>0.10</b>	0.10	%
Gun tim. jitter	Δt <sub>0</sub>	0.15	<b>0.15</b>	0.15	psec
Initial charge	ΔQ/Q	4.00	<b>4.00</b>	4.00	%

Table 4: RF phases per sector

L0	L1	LX	L2	L3	L4
φ0=0	φ1=-30 (-20)	φX=-150	φ2=-30	φ3=-32	φ4=0

*RF Measurements*

In order to be able to assess the stability of the existing systems, we did preliminary phase jitter measurements using the same procedure as in the MIT-BATES measurements setup [8]. The two labs use different types of RF transmitter and this allows us to compare the behavior of the two systems: the one at MIT-Bates, based upon a hard tube modulator and solid state switch, without a step-up transformer, and that at ELETTRA, based upon a PFN, thyratron and pulse transformer.

While operating at 10 Hz, we tested four of the existing systems at ELETTRA (MK3, MK4, MK5 and MK7) observing the pulse to pulse variation of the mean (integrated) phase in the range of 1 sec. to 10 min. (10 to 6000 pulses). The measurement setup is shown in Fig. 2, and it is followed by the list of the components used in the measurement. As one can see from the figure, the measurement tried to characterize the systems' components, from the klystron to the complete system, including the accelerating section. The phase noise measurement has been carried out over 1 μsec from the 3.0 μsec total RF pulse length.

Fig. 3 shows the scope trace relative to the acquisition of 3000 pulses on the klystron in the MK5 section: over 5 min. of statistics, the pulse to pulse integrated phase variation is below 0.06 °S.

The results obtained from the configurations reported in the scheme of Fig. 2, are summarized in Table 5. The last column for each configuration shows the average values over the four stations. Acquisition problems resulted in the missing data for the klystron (A-1) 10 min. period.

A preliminary analysis shows that the pulse to pulse variation of the mean phase remain within acceptable levels; for example, the klystron (A-1) stays within  $0.04^\circ\text{S}$  over 1 sec. (10 pulses), reaching  $0.06^\circ\text{S}$  in 5 min. (3000 pulses). The same values vary between  $0.15^\circ\text{S}$  and  $0.6^\circ\text{S}$  for the whole system, requiring a feedback system capable of keeping the transmitters within the LiTrack requirements.

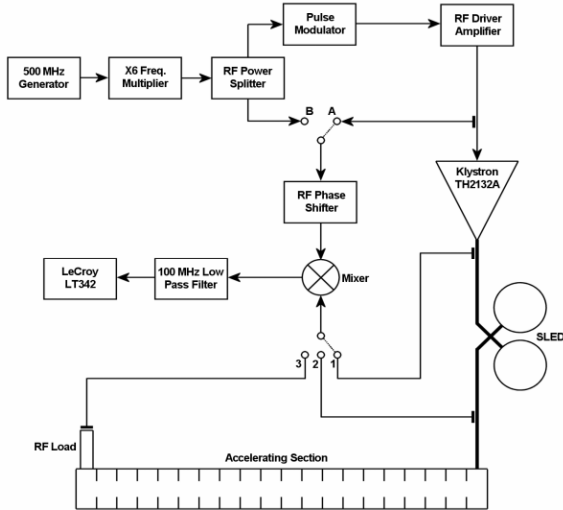


Figure 2: phase jitter measurement layout

The experimental setup was implemented with the following key components:

- 500 MHz Gen.: Rohde & Schwarz SMG-B1 (opt. Osc.);
- X6 Freq. Mult.: Nucltudes TRI 270 +STG800 filter;
- RF Power Splitter: Mini Circuit ZAPD-4;
- Pulse Mod.: Mini Circuit ZYSWA-2-50DR;
- RF Driv. Ampl.: Nucltudes M.30.50.190 PS;
- RF Phase Shifter: Flann 10063;
- Mixer: Mini Circuit ZEM-4300
- 100MHz Lowpass Filter: Mini Circuit BLP-100
- Oscilloscope: Lecroy Waverunner LT342

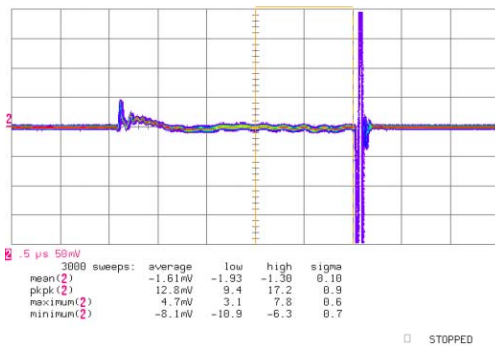


Figure 3: MDK5 Klystron 1 µsec averaged phase noise (3000 pulses, 5 minutes)

**RF Measurements at MIT-Bates**

In preparation for the systems tests in Trieste, we performed a full set of measurements on the MIT-Bates linac (transmitter No. 6). We have used the existing Phase

and Amplitude Monitoring [9], with a multi channel triggered 16 BIT ADC to acquire numerous parameters such as temperature and DC high voltage. A gated integrator was used to simultaneously sample and hold pulsed signals such as anode voltage and current, and output phase and amplitude. A passive mixer array was implemented: four mid level S band mixers outputs were summed together. A dial vernier phase shifter (Narda 3752) was used to calibrate the output. This signal was routed to an oscilloscope with extensive statistics functions (LeCroy LT344). The Bates phase jitter measurements show mostly uncorrelated phase noise at all frequencies as shown in the spectrum analyzer trace below.

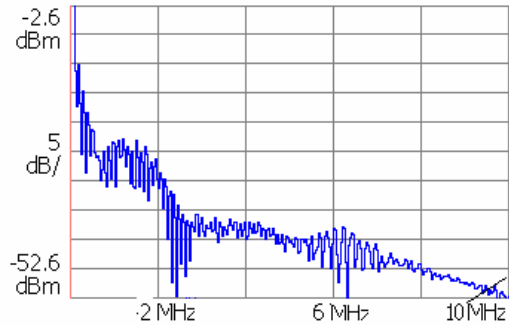


Figure 4: phase noise spectrum

The peak to peak high frequency phase jitter results were typically  $\sim 1.1^\circ\text{S}$ , when we measure  $6\mu\text{s}$  of a total RF pulse length of  $10\mu\text{s}$ . Over the  $\sim 60$  seconds of statistics the pulse to pulse integrated amplitude and phase variation is  $1.61\text{mV RMS}$  and  $0.07^\circ\text{S RMS}$  respectively. Fig. (5) shows an oscilloscope trace of the phase detector output of the  $10\mu\text{s}$  wide drive klystron pulses phase versus the reference/drive line phase.

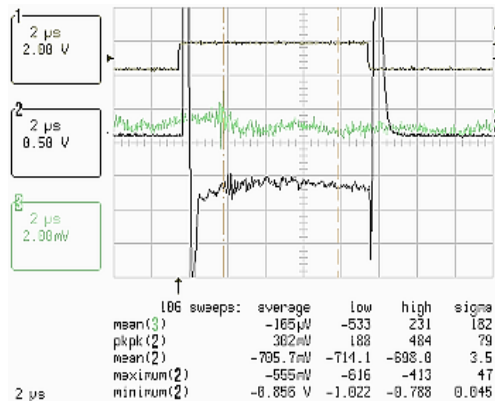


Figure 5: 10 µsec phase behaviour

The calibration is  $0.0062^\circ/\text{mV}$  near the null. The peak to peak phase jitter results per single pulse were also typically  $\sim 1^\circ\text{S}$ . Over the 100 pulses ( $\sim 3$  sec.) of statistics the pulse to pulse integrated phase variation is  $3.5\text{ mV RMS}$  or  $0.02^\circ\text{S RMS}$ .

### 3. THE NEW RF CONTROLLER

We have selected to adopt an FPGA based, digital controller, such as that which has been successfully demonstrated in the SNS linac controller [10]. The digital approach can be very effective in correcting errors. Its tight integration with the software system make it ideally suited for corrections of slow errors from a fraction of a second to long term drifts. Its internal processing allows for fast advanced correction schemes, such as adaptive feed-forward, with a high degree of accuracy. Due to the pulse length of the system, it is nearly impossible to have an effective feedback system within the pulse, since the propagation delay in the loop is comparable to the pulse length. We are therefore planning to exploit feed-forward and adaptive feed-forward to minimize pulse to pulse fluctuations. It is also important to note that since in FELs the bunch length is extremely short compared to the RF pulse, pulse-to-pulse repeatability at the time of arrival of the bunch is the dominant parameter: pulse flatness is not so critical as long as each bunch arrives at the same instant in amplitude and phase. This makes the integration of the RF controller with the synchronization system an essential element of the successful design. A picture of the LBNL RF controller built for SNS is shown in Fig. 6.

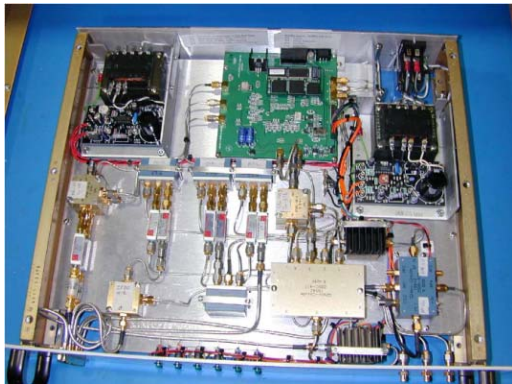


Fig. 6: LBNL RF controller

### CONCLUSIONS

A brief overview of the current ELETTRA linac, mainly focused on the performance of the RF systems, has been given.

Preliminary simulation results using LiTrack have been carried out to evaluate the sensitivity and tolerance needed by the RF system in the FERMI proposed layout, with respect to the phase and amplitude requirements. These studies demonstrate that the specified values are within reach of the present technology. Early phase jitter measurements, performed on four RF plants operating on the present machine, are encouraging and show that the required performance is reachable with an upgrade of the systems that include, in particular, the installation of a new RF feedback system and the improvement of some key components. Further simulations and more extensive tests and measurements are already planned in the near future.

Table 5: main phase pulse to pulse rms variation ( $^{\circ}$ S)

	MK3	MK4	MK5	MK7	AVG
<b>Klystron (pos: A-1)</b>					
<b>1 sec</b>	0.031	0.048	0.034	0.019	0.033
<b>5 sec</b>	0.036	0.048	0.034	0.030	0.037
<b>10 sec</b>	0.036	0.037	0.034	0.034	0.035
<b>30 sec</b>	0.036	0.070	0.038	0.030	0.043
<b>1 min</b>	0.041	0.092	0.041	0.030	0.051
<b>5 min</b>	0.056	0.088	0.038	0.049	0.058
<b>10 min</b>	-	-	-	-	-
<b>Driver-Klystron (pos: B-1)</b>					
<b>1 sec</b>	0.056	0.038	0.049	0.034	0.044
<b>5 sec</b>	0.067	0.038	0.053	0.060	0.055
<b>10 sec</b>	0.056	0.042	0.057	0.053	0.052
<b>30 sec</b>	0.078	0.069	0.057	0.060	0.066
<b>1 min</b>	0.111	0.046	0.064	0.056	0.069
<b>Time</b>	0.108	0.080	0.200	0.060	0.112
<b>10 min</b>	0.130	0.096	0.230	0.120	0.144
<b>Driver-Klystron-SLED detuned (pos: B-2)</b>					
<b>1 sec</b>	0.045	0.069	0.071	0.069	0.064
<b>5 sec</b>	0.068	0.061	0.056	0.084	0.067
<b>10 sec</b>	0.057	0.058	0.060	0.065	0.060
<b>30 sec</b>	0.079	0.061	0.060	0.084	0.071
<b>1 min</b>	0.090	0.088	0.056	0.126	0.090
<b>5 min</b>	0.188	0.104	0.075	0.168	0.134
<b>10 min</b>	0.354	0.561	0.188	0.172	0.319
<b>Driver-Klystron-SLED detuned-Section (pos: B-3)</b>					
<b>1 sec</b>	0.153	0.169	0.177	0.098	0.149
<b>5 sec</b>	0.138	0.184	0.162	0.184	0.167
<b>10 sec</b>	0.181	0.157	0.181	0.162	0.170
<b>30 sec</b>	0.169	0.184	0.211	0.218	0.196
<b>1 min</b>	0.173	0.184	0.238	0.169	0.191
<b>5 min</b>	0.358	0.338	1.076	0.237	0.502
<b>10 min</b>	0.634	0.441	1.027	0.335	0.609

### ACKNOWLEDGMENTS

The authors would like to acknowledge the precious contributions of Paul Emma, for many inspiring conversations and the help with LiTrack. In addition, we want to acknowledge the support of Defa Wang, and Brian McAllister for their help while measuring the systems at MIT-Bates, and the ELETTRA linac group for their support in the measurements at Trieste.

### REFERENCES

- [1] C. J. Bocchetta et al., "FERMI @ Elettra: a Seeded Harmonic Cascade FEL for EUV and Soft X-Ray", these proceedings.
- [2] G. D'Auria et al., "Operation and status of the Elettra Injector Linac", PAC '97, Vancouver, B.C., Canada, May 1997, p. 1212.
- [3] S. Di Mitri et al., "Optimization and modeling of the accelerator for the FERMI@ELETTRA FEL", these proceedings.
- [4] S. M. Lidia et al., "The RF Injector for the FERMI@ELETTRA Seeded X-ray FEL", these proc.
- [5] S. Di Mitri et al., ST/F-TN-05/01
- [6] G. D'Auria et al., ST/F-TN-05/07
- [7] K. Bane et al., SLAC-PUB-11035
- [8] D. Cheever et al., Mit-Bates RF Meas. June 2005.
- [9] D. Cheever et al., "The Bates Phase and Amplitude Monitoring System", ICALEPS 2001.
- [10] L. Doolittle et al., "The design and performance of the Spallation Neutron Source Low-Level RF Control System", LINAC '04, Luebeck, DE, August 2004, pag 704.